Sensors & Diagnostics

CRITICAL REVIEW

View Article Online
View Journal | View Issue

Check for updates

Cite this: *Sens. Diagn.*, 2024, **3**, 1789

Point-of-care biosensors and devices for diagnostics of chronic kidney disease

Yuan Liu,*[abc] Xinping Zhao,[bc] Min Liao,[bc] Guoliang Ke *[a] and Xiao-Bing Zhang [a]

Chronic kidney disease (CKD) is a growing global health concern, necessitating early and accurate diagnostic tools to manage and mitigate its progression. Point-of-care (POC) biosensors and devices offer a promising solution for rapid, cost-effective, and accessible diagnostics. This review explores the latest advancements in POC biosensors and devices specifically designed for CKD diagnostics. In this review, we discuss the biosensors most likely to achieve on-site detection of CKD, focusing on their design and application in real samples, including electrochemical, fluorescent, and colorimetric sensors. Also, the innovative platforms are summarized from lateral flow devices, lab-on-a-chip devices, and microfluidic-based devices. The potential of these technologies for real-time monitoring, early detection, and personalized treatment is underscored. The review concludes by envisioning future perspectives and the transformative impact of POC biosensors in CKD diagnostics, aiming to improve patient outcomes and healthcare efficiency.

Received 2nd July 2024,
Accepted 13th September 2024

DOI: 10.1039/d4sd00241e

rsc.li/sensors

Open Access Article. Published on 16 September 2024. Downloaded on 2/10/2026 6:27:48 AM.
This article is licensed under a Creative Commons Attribution-NonCommercial 3.0 Unported Licence.

1. Introduction

Chronic kidney disease (CKD) has become a global public health problem. It is a progressive condition characterized by the gradual loss of kidney function over time, often resulting in end-stage renal disease (ESRD) if not effectively managed. CKD is associated with numerous complications, including cardiovascular disease, hypertension, anemia, and electrolyte imbalances, which significantly impact patients' quality of life and increase healthcare costs.[1,2] According to the Global Burden of Disease study, CKD is one of the leading causes of morbidity and mortality worldwide, with an estimated prevalence of 10% globally. The global kidney function diagnostics market, valued at $850 million in 2022, is projected to expand significantly, reaching $1.39 billion by 2030. Hence, early detection and continuous monitoring are critical for managing CKD and preventing its progression to more severe stages.

CKD diagnosis typically relies on several clinical benchmarks, primarily focused on assessing kidney function and damage, such as glomerular filtration rate (GFR), serum creatinine, albuminuria, histopathology and imaging studies. Specific types of CKD have different underlying causes, which

[a] *State Key Laboratory for Chemo/Biosensing and Chemometrics, College of Chemistry and Chemical Engineering, Hunan University, Changsha, 410082, China. E-mail: gxuliuyuan@163.com, glke@hnu.edu.cn*
[b] *Institute of Cytology and Genetics, School of Basic Medical Sciences, Hengyang Medical School, University of South China, Hengyang, 421001, China*
[c] *Institute for Future Sciences, University of South China, Changsha, 410000, China*

Yuan Liu

Yuan Liu received her PhD degree from Southeast University in 2022. She then joined the University of South China in the same year. She has pursued her research as a Postdoctoral Researcher at the Hunan University from 2023 to the present. Her research focuses on bioanalysis and the application of functional nano-probes in nucleic acid biosensors.

Xinping Zhao

Xinping Zhao earned her bachelor's degree from Hunan University of Science and Technology in 2023 and is currently studying for her Master's degree in Biology at the University of South China under the tutelage of Prof. Liu Yuan. Her research interests are mainly in biosensors.

© 2024 The Author(s). Published by the Royal Society of Chemistry

Open Access Article. Published on 16 September 2024. Downloaded on 2/10/2026 6:27:48 AM. This article is licensed under a Creative Commons Attribution-NonCommercial 3.0 Unported Licence.

are reflected in their specific clinical aims and the biomarkers targeted for diagnosis, monitoring, and treatment. The primary causes of CKD associated with various biomarkers as well as the diagnostic methods are shown in Fig. 1. Traditionally, CKD diagnosis and monitoring rely on laboratory-based tests such as the measurement of serum creatinine, blood urea nitrogen (BUN), and urinary albumin and the estimation of the GFR or urine albumin-to-creatinine ratio (ACR).[3] While these methods are accurate, well-established and reliable, they often require sophisticated equipment, trained personnel, and multiple patient visits and can be time-consuming, making them less accessible in remote or resource-limited settings.[4] Additionally, these methods can be inconvenient for patients, leading to delayed diagnosis and treatment. Consequently, there is a growing need for more accessible and efficient diagnostic solutions.[5]

Recent innovations have led to the creation of highly sensitive and specific biosensors capable of detecting low concentrations of CKD biomarkers in breath gas[6] and bodily fluids such as blood, urine, and saliva.[7,8] According to the detection mechanisms, the biosensors can be divided into fluorescent-based, surface-enhanced Raman scattering (SERS)-based, colorimetric-based, electrochemical-based, and surface plasmon resonance (SPR)-based biosensors.

Since the growing interest in POC biosensors is driven by the need for more accessible and cost-effective diagnostic solutions that can be deployed in a variety of settings, including primary care clinics, remote areas, and even home monitoring,[9–11] POC biosensors and devices utilizing electrochemical, optical, and microfluidic techniques to measure CKD biomarkers have become the research hotpots in the clinic.[12] Even though SPR and SERS biosensors have indeed improved sensitivity and selectivity, they are still difficult to use in POC testing.[13,14] The details of some commercialized POC devices based on electrochemical or optical technologies for the diagnostics of CKD are listed in Table 1. POC biosensors and devices are often designed to provide rapid, accurate, and on-site diagnosis and monitoring of biological markers associated with CKD. The development of POC biosensors for CKD has seen several important milestones, from the early urine dipstick tests, POC creatinine meters, multiplexed microfluidic devices, wearable kidney function monitors, smartphone-integrated POC devices, to POC biosensors for novel biomarkers, reflecting advances in technology and diagnostic capabilities. Moreover, by reducing the reliance on centralized laboratory facilities and providing immediate results, POC devices have the potential to significantly improve the diagnosis and management of CKD, particularly in underserved populations.[15] Furthermore, the integration of these sensors with wireless communication and data analysis platforms enables seamless data transfer and remote monitoring, facilitating timely medical intervention and personalized treatment strategies.[16] As a result, there has emerged a

Min Liao

Min Liao is currently studying for her bachelor's degree in Clinical Medicine at the University of South China from 2022 to the present. Her research interest focuses on detection of tumor biomarkers using fluorescence biosensors.

Guoliang Ke

Guoliang Ke is a Professor in the Department of Chemistry at Hunan University. He received his BS degree in 2010 and PhD degree in 2016, both from Xiamen University, and visited Arizona State University during 2013–2015. His research focuses on DNA nanotechnology based biosensing, bioimaging, and cancer therapy.

Xiao-Bing Zhang

Xiao-Bing Zhang is a Professor in the Department of Chemistry at Hunan University. He completed his BS degree in 1993 and PhD degree in 2001, both in Chemistry from Hunan University. He worked at the Ecole Normale Superieure de Lyon (France) and the Royal Institute of Technology (Sweden) as a postdoctoral fellow from 2003 to 2005. He served as an invited professor at ENS de Lyon in 2008 and as a visiting professor at the University of Illinois at Urbana-Champaign in 2009. Professor Zhang's research interests include bioimaging and biosensing.

© 2024 The Author(s). Published by the Royal Society of Chemistry

Open Access Article. Published on 16 September 2024. Downloaded on 2/10/2026 6:27:48 AM. This article is licensed under a Creative Commons Attribution-NonCommercial 3.0 Unported Licence.

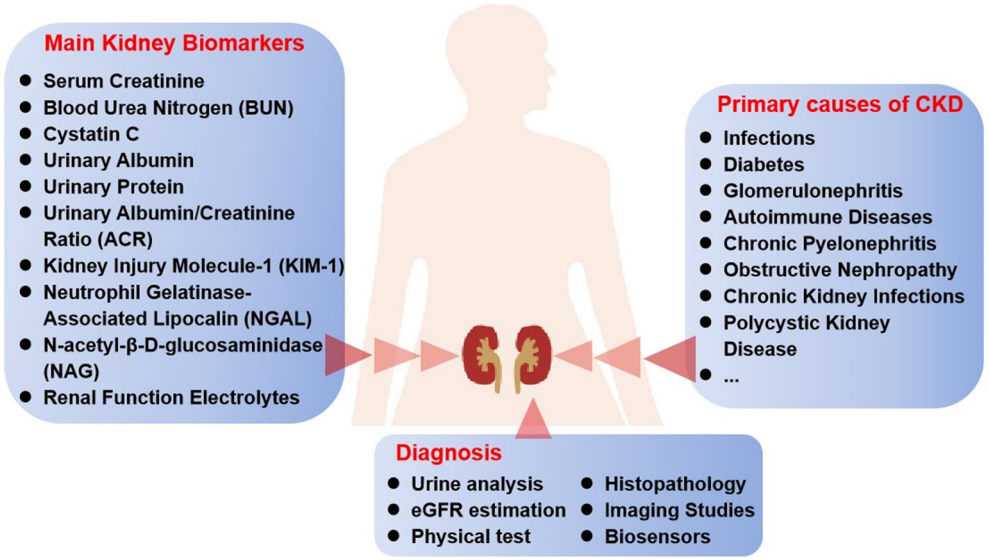

Fig. 1 Primary causes, main biomarkers and diagnostic methods of chronic kidney disease.

research highlight in POC biosensors or devices for the detection of CKD and many of them show great potential in practical utilization. However, there are still many challenges to be addressed before they come to commercialization in this field. In this circumstance, a comprehensive review is needed to summarize the recent progress and present insights to address those problems and promote the transformation of POC biosensors and devices into practical applications. Although there have been several reviews related to this topic in the past years, most of them are either not up to date or not focused on both POC biosensors and devices.[17–21] For example, Tricoli *et al.* reviewed the earlier

Table 1 The details of some commercialized POC devices based on electrochemical or optical technologies for the diagnostics of CKD

Devices	Technologies	Target analytes	LODs	Merits	Limitations
Abbott i-STAT system	Electrochemical sensor	Creatinine, BUN, electrolytes (sodium, potassium)	Creatinine: 0.2 mg dL^{-1} BUN: 2 mg dL^{-1} Sodium: 5 mmol L^{-1} Potassium: 0.2 mmol L^{-1}	Handheld and portable; provides results within minutes, facilitates quick clinical decisions	Lower accuracy and sensitivity
Piccolo Xpress	Microfluidic & absorbance photometry	Creatinine, BUN, glucose, electrolytes (sodium, potassium, chloride)	Creatinine: 0.2 mg dL^{-1} BUN: 2 mg dL^{-1} Glucose: 2 mg dL^{-1} Sodium: 5 mmol L^{-1} Potassium: 0.2 mmol L^{-1} Chloride: 5 mmol L^{-1}	Rapid results; ease of use; comprehensive testing	Higher cost
Siemens CLINITEK Status+	Reflectance photometry	Albumin, creatinine, protein, glucose in urine	Albumin: 10 mg L^{-1} Creatinine: 10 mg dL^{-1} Protein: 6 mg dL^{-1} Glucose: 50 mg dL^{-1}	Rapid results; ease of use; quick for screening albuminuria	Single sample type, limited quantitative precision, lower sensitivity
Nova Biomedical StatSensor	Electrochemical sensor	Serum creatinine	0.3 mg dL^{-1}	Highly portable, suitable for use in emergency settings and operating rooms; rapid results	Limited to creatinine measurement

© 2024 The Author(s). Published by the Royal Society of Chemistry

Open Access Article. Published on 16 September 2024. Downloaded on 2/10/2026 6:27:48 AM. This article is licensed under a Creative Commons Attribution-NonCommercial 3.0 Unported Licence.

work of miniaturized bio-and chemical-sensors for POC monitoring of CKD in 2018.[17] A recent review by Gama *et al.* was focused on utility, accuracy, and acceptability of the roles of POCT in CKD.[20]

Herein, this review aims to provide a timely and comprehensive overview of the current state of POC biosensors and devices for CKD diagnostics. It will cover the technological principles behind these innovations, recent developments in the field, and their potential impact on clinical practice. Additionally, the review will discuss the challenges and limitations associated with the adoption of POC technologies and propose future directions for research and development.

2. The detection methods for CKD diagnostics

The methods for CKD detection are crucial due to their ability to provide rapid, accurate, and minimally invasive diagnostics. With the development of technology, the biosensor-based approach can facilitate not only early detection but also continuous monitoring for CKD patients.[22] Thus, in this section, the recent progress of the biosensor-based methods most likely to achieve on-site detection of CKD are systematically summarized, including electrochemical biosensors, fluorescent biosensors, and colorimetric biosensors.

2.1 Electrochemical biosensors

Electrochemical biosensors leverage the specificity of biological recognition mechanisms and the sensitivity of electrochemical measurements to provide real-time, accurate detection of diverse substances. During the past decade, electrochemical biosensors have been widely studied owing to their advantages of rapid response, portability, high specificity, and miniaturization, which make them ideal for POC settings.[23] Electrochemical biosensors can be classified into voltammetric-based biosensors, amperometric-based biosensors, conductometric-based biosensors, impedimetric-based biosensors and potentiometric-based biosensors according to the electrochemical conduction mode. As for CKD biomarker detection, the mostly used methods are the first three kinds. Potentiometric-based biosensors are often used to measure ion concentrations, such as potassium or sodium, which are critical for monitoring kidney function.

2.1.1 Voltammetric-based biosensors. Voltammetric-based biosensors represent a sophisticated class of electrochemical sensors used for the detection and quantification of various analytes.[24] These sensors leverage voltammetry, a technique that measures the current as a function of an applied potential, to provide detailed information about the electrochemical properties of the analyte. There are several types of voltammetric techniques that can be employed, each offering unique advantages depending on the application, such as cyclic voltammetry (CV), which is useful for studying the redox properties and kinetics of analytes; differential pulse voltammetry (DPV), which applies a series of potential pulses and measures the current at the end of each pulse, offering high sensitivity and resolution; square wave voltammetry (SWV), which uses square-shaped potential pulses, providing high sensitivity and rapid analysis.[25]

For instance, Bajpai *et al.* reported a simple voltammetric biosensor for the detection of creatinine in artificial urine samples using unmodified glass carbon electrodes (GCEs) and screen-printed carbon electrodes (SPCEs). The CV curves showed that the ferrocyanide oxidation peak was increased linearly with the concentration of creatinine. After optimization, this alkaline ferrocyanide non-enzymatic electrochemical biosensor showed high sensitivity to creatinine with linear detection concentrations of 0.2–2.14 mM using a GCE and 0–18 mM using a SPCE, and the limit of detection was 65 μM and 60 μM, respectively.[26] To improve the detection sensitivity, various nanomaterials (NMs) were used to modify the electrodes, due to their unique properties at the nanoscale, such as excellent electrical conductivity and high specific surface area.[27] For example, Wang *et al.* fabricated a multi-parameter voltammetric biosensor based on electropolymerized PANI:PSS/AuNPs/SPCE for the detection of ammonium ions (NH^{4+}), urea, and creatinine. In this biosensor, the AuNPs were modified on the SPCE to increase the sensor reaction surface area, and hence to improve the electron transfer efficiency. Later, the PANI:PSS film was electropolymerized on the surface of AuNPs/SPCE as an NH^{4+} sensitive material. Then urease and creatinine deiminase were modified to the PANI:PSS/AuNPs/SPCE surface to form a urea- and creatinine-sensing platform. Besides, the electrodes were integrated into a paper-based device to detect multiple biomarkers in real human urine samples, demonstrating that the multi-parameter biosensor is a promising candidate for POC testing of urine for CKD management.[28] To further enhance the sensitivity of electrochemical biosensors, Saeed *et al.* designed a CoTe nanorod modified GCE biosensor for the determination of albumin in urine *via* CV. Specifically, CoTe nanorods with large surface area and effective electron transfer characteristics were often used to act as conductive materials. Thus, the oxidation–reduction peaks in CV were greatly improved and the detection limit was improved to 0.09 nM.[29] Meanwhile in another study, a novel nanostructure ZIF-8-$Cu_{1-x}Ni_x(OH)_2$@Cu/PEDOT:PSS/ITO was developed for the determination of cystatin C. In this system, the ZIF-8-$Cu_{1-x}Ni_x(OH)_2$@Cu NPs with bimetallic Cu–Ni composites showed excellent electrocatalytic activity, further coated with anti-cystatin C. Thus, a highly sensitive nano-immunosensor was constructed due to the great improvement of electrochemical performance, and the detection limit was nearly 33 pg mL^{-1} by the DPV technique.[30]

Molecularly imprinted polymers (MIPs) offer a powerful and versatile approach to creating synthetic receptors with

© 2024 The Author(s). Published by the Royal Society of Chemistry

Open Access Article. Published on 16 September 2024. Downloaded on 2/10/2026 6:27:48 AM.
This article is licensed under a Creative Commons Attribution-NonCommercial 3.0 Unported Licence.

high specificity and affinity for target molecules. Their robustness, reusability, and cost-effectiveness make them suitable for a wide range of applications, including sensors and separation techniques. For example, Saddique *et al.* reported a highly sensitive creatinine–MIP biosensor based on a metal oxide (MOx) nanocrystal modified SPCE. MIPs were used for specific recognition of creatinine molecules and MOx with good electrical conductivity was used to enhance the sensitivity of the electrochemical biosensor. Thus, a limit of detection of 90 nM was obtained.[31] Usually the electrode can achieve multiple detection *via* molecular imprinting with different targets. For example, Wardani *et al.* developed a MIP dual biosensor based on carboxylated multiwalled carbon nanotube (fMWCNT) modified SPCEs for the one-step detection of ACR. In this assay, the SPCE electrodes were molecularly imprinted with creatinine and albumin template molecules for specific recognition of dual biomarkers. With the modification of fMWCNTs, the performance of the proposed MIP dual biosensor could be significantly improved.[32]

Although the sensitivity of these sensors is improved, the modification of other materials can further increase the sensitivity. Recently, Saeed *et al.* developed a creatinine–MIP POC diagnostic electrochemical biosensor based on an exfoliated graphitic carbon nitride nanosheet (gCN) modified electrode for the timely detection of creatinine in saliva (Fig. 2A). Nanozymes composed of gCN and miPTh were synthesized to enhance the electron exchange at the

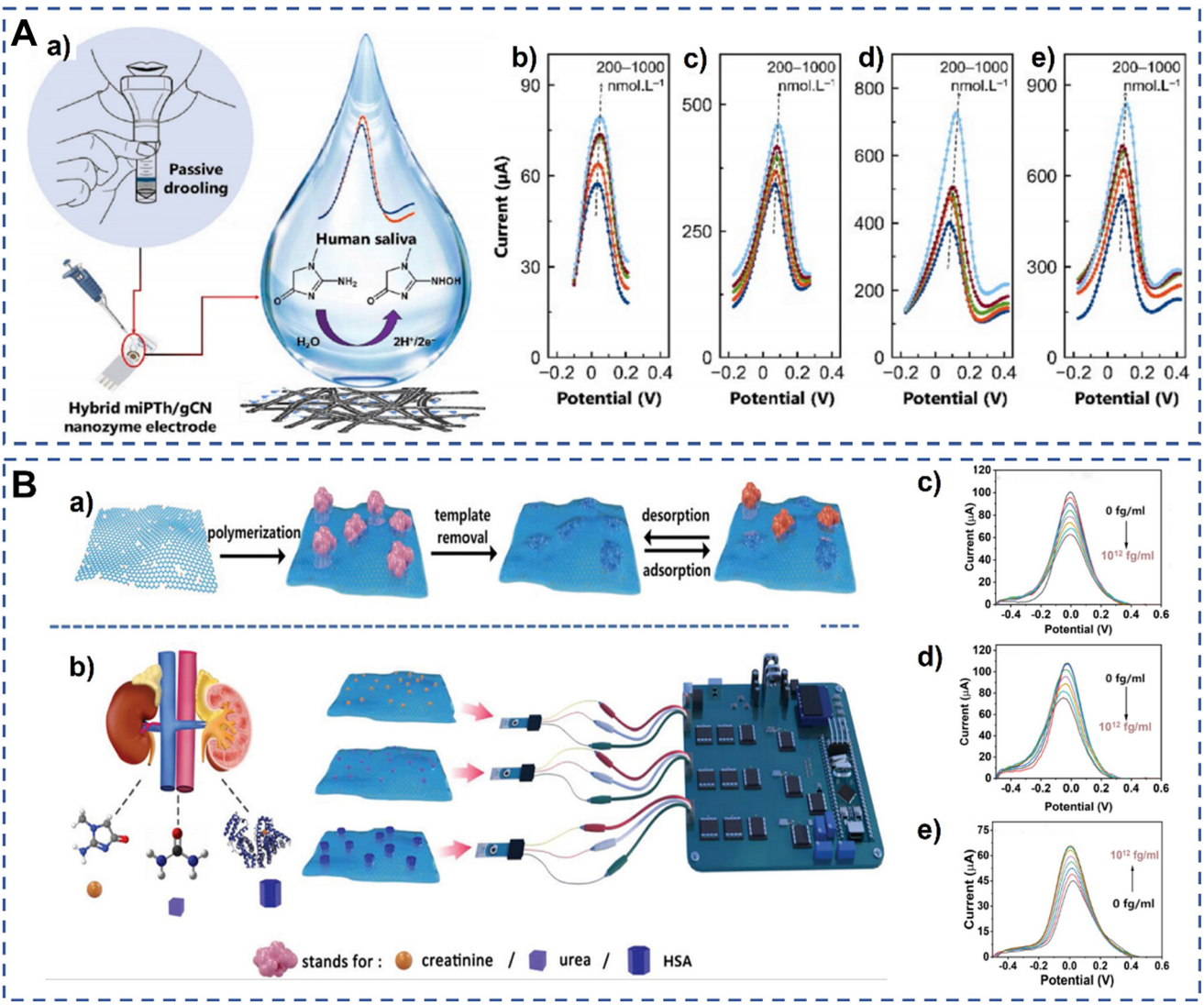

Fig. 2 Schematic illustration of voltammetric electrochemical biosensors for detection of CKD biomarkers. (A) A schematic of salivary creatinine monitoring (a) and the DPV response of (b) niPTh, (c), miPTh, (d) niPTh/gCN, and (e) miPTh/gCN nanozyme sensors toward different concentrations of creatinine in a standard redox solution.[33] Copyright 2023, Elsevier. (B) Overview of the surface-MIP synthesis and its detection process based on the designed multiplexed POC sensing platform for the simultaneous detection of creatinine, urea, and HSA. (a) The preparation and recognition process of surface-MIP (rGO/PDA-MIP) composites. (b) Workflow of the simultaneous detection of biomarkers using an MIP-based electrochemical sensor with self-designed POC readout. The corresponding DPV responses of rGO/PDA-MIP modified electrodes to different concentrations of creatinine (c), urea (d), and HAS (e) in the electrolyte.[34] Copyright 2024, Wiley.

© 2024 The Author(s). Published by the Royal Society of Chemistry

Open Access Article. Published on 16 September 2024. Downloaded on 2/10/2026 6:27:48 AM. This article is licensed under a Creative Commons Attribution-NonCommercial 3.0 Unported Licence.

nanozyme–electrolyte interface and to improve the selectivity to creatinine. The fabricated miPTh/gCN biomimetic nanozyme based biosensor exhibited better electrocatalytic properties, and its electrochemical properties were investigated by DPV. After optimization, this biosensor showed an excellent response to creatinine detection with the limit of detection of 340 pM.[33] Besides, Li *et al.* developed a multiplexed MIP electrochemical biosensor for simultaneous determination of creatinine, urea and HSA (Fig. 2B). Reduced graphene oxide/polydopamine (rGO/PDA) with enhanced surface area was used to modify the working electrode, which could facilitate the rapid electron transfer on the electrode surface. Thus, the detection platform showed high sensitivity for the direct measurements of creatinine, urea and HSA in clinical serum and urine samples. After optimization, the detection limits reached 0.27, 3.87, and 0.52 fg mL^{-1} for creatinine, urea and HSA, respectively. Moreover, the electrodes were integrated into a miniaturized device, showing potential for early POC CKD diagnosis.[34]

2.1.2 Amperometric-based biosensors. Amperometric-based biosensors are a type of electrochemical biosensor that measures the current produced by the oxidation or reduction of an electroactive species at an electrode surface. The current is directly proportional to the concentration of the target analyte, making amperometric-based biosensors highly sensitive and suitable for quantitative analysis.[35] For example, Chen *et al.* developed a low-cost amperometric biosensor for the detection of ammonia. This organic gas biosensor exhibited a great increase in operational current after using F4-TCNQ as a P-type in comparison with the non-doped biosensor. F4-TCNQ with a higher hole mobility and lower hole injection barrier made the circuitry sensing system a candidate for POC detection.[36]

Similar to voltammetric-based biosensors, amperometric-based biosensors also need a variety of NMs to increase sensitivity. Metal–organic frameworks (MOFs), a three-dimensional structure, have unique cavities and adjustable pore size to hold targets, making them highly versatile for sensing applications. For example, Banga *et al.* used a faradaic probe embedded into a MOF cavity for noninvasive ammonia detection (Fig. 3). Zinc-imidazole framework 8 (ZIF-8) was used to accommodate ammonia and further protect targets from major external stimuli. Ferrocene (Fc) was used in electrocatalysis for oxygen reduction to provide the current signal. The good performance of the electrochemical properties demonstrated that this bifunctional probe (Fc@ZIF-8) based sensing system can serve as a promising platform for POC diagnostics.[37] Later, this team developed an innovative amperometric biosensor for the detection of ammonia. Unlike the previous biosensor, this amperometric biosensor used activated carbon as a signal transducer.[38]

To fabricate a urea sensor, Vega *et al.* developed a Ni-based MOF sensing platform. The Ni atoms encapsulated into the MOF could enhance the catalytic activity. Hence, a competitive amperometric biosensor was designed to detect urea *via* the urea electro-oxidation reaction, and the limit of detection was 3.5 μM.[39] In another study, Promphet *et al.* reported a wearable biosensor for non-invasive detection of sweat urea. In this sensor, silk was chosen as a wearable skin patch, and its conductivity could be enhanced by AuNPs. Thus, a non-invasive amperometric biosensor with high electrical conductivity and biocompatibility was designed, which offered a linear range of 0–100 mM with a detection limit of 20 mM.[40] To realize multiplex detection, Liu *et al.* developed a biosensing array modified with different enzymes for simultaneous detection of glucose, creatinine and uric acid. Thus, the biosensor can linearly detect the three biomarkers in plasma ranging from 0.5 to 18 mM, 0.04 to 1 mM, and 0.04 to 0.8 mM, respectively.[41]

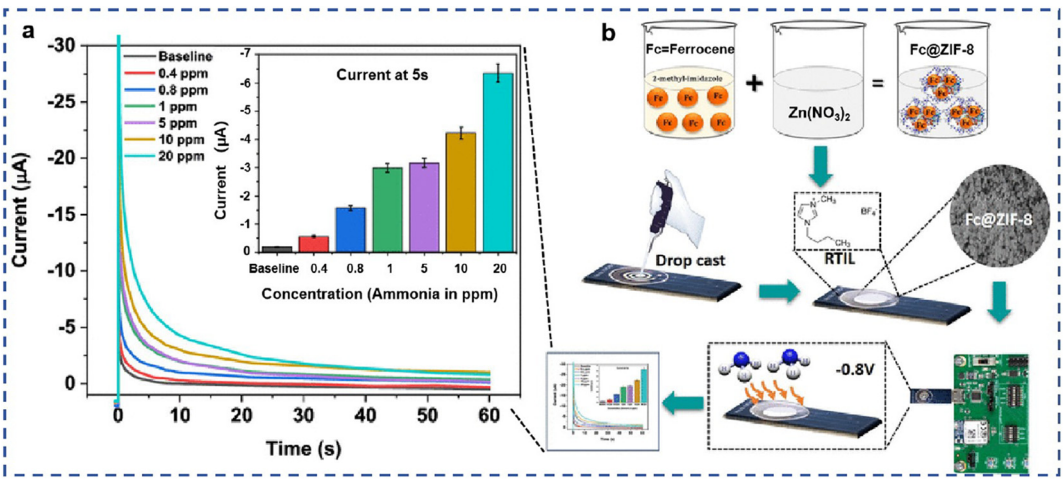

Fig. 3 Schematic illustration of amperometric electrochemical biosensors for ammonia detection. (a) Diffusion-limited chronoamperometry. Calibrated dose–response chronoamperograms for ammonia gas concentration ranging from 400 ppb to 20 ppm. (b) Schematic representation of the optimized preparation approach of Fc@ZIF-8-modified SENCE.[37] Copyright 2021, American Chemical Society.

© 2024 The Author(s). Published by the Royal Society of Chemistry

Open Access Article. Published on 16 September 2024. Downloaded on 2/10/2026 6:27:48 AM.
This article is licensed under a Creative Commons Attribution-NonCommercial 3.0 Unported Licence.

2.1.3 Conductometric-based biosensors. Conductometric-based biosensors are a type of electrochemical biosensor that measures changes in the electrical conductivity of a solution as a result of a biochemical reaction. These biosensors leverage the principle that the presence or concentration of specific analytes can alter the ionic composition and conductivity of the medium. Hence, conductometric biosensors are often used to detect metabolites like glucose and urea. Besides, conductometric biosensors represent a powerful and versatile tool in diagnostics, offering rapid, sensitive, and specific detection of a wide range of analytes in various applications. As a paradigm, Lee *et al.* reported a soft candy-based sensor for salivary electrical conductivity diagnosis of CKD risk. The soft candy-based conductometric biosensor without consistent wetting could lead to misdiagnosis. Hence, the traditional wetting strategies cannot meet the demand. In this case, multiple measuring points were designed and sequential measurements between them were performed (Fig. 4).[42] Under optimal conditions, the designed conductometric biosensor showed a detection limit of 0.01 M (206 μS cm^{-1}), which showed better performance than their previous work.[43] Moreover, the conductometric biosensor showed a conductivity of ~3535 μS cm^{-1} in human saliva tests, while a healthy adult has a salivary conductivity of ~3500 μS cm^{-1} and that of a CKD patient is above ~13 000 μS cm^{-1}.[42] Hence, the

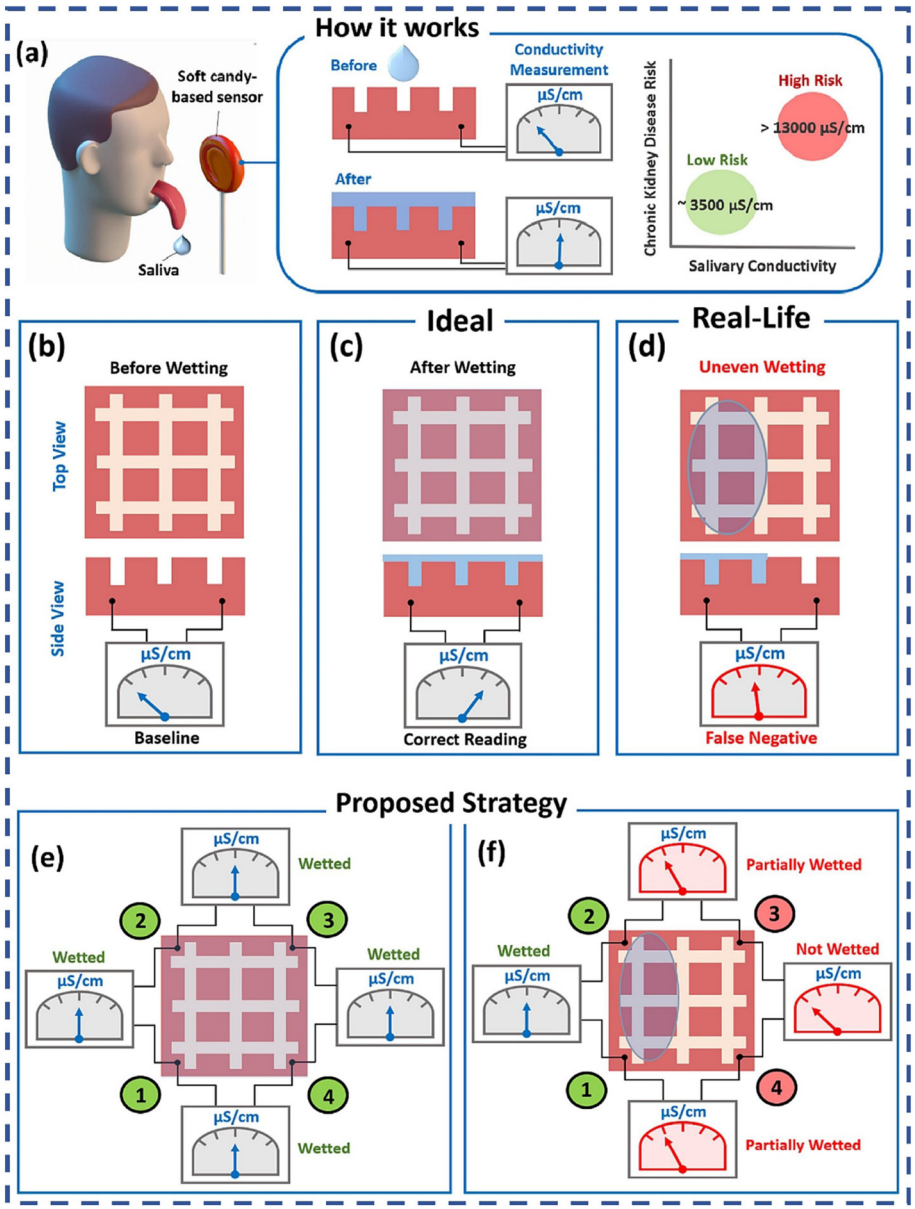

Fig. 4 Challenges of the soft candy-based conductometric biosensor and proposed multiplexing to circumvent them: (a) soft candy-based sensor operating principle; ideal operating scenarios: (b) before wetting; (c) after wetting; real-life operating scenarios: (d) uneven wetting of the sensor surface; proposed multiplexing strategy: (e) before wetting; (f) detection of uneven wetting, relays 1, 2, 3, and 4 are to connect pads 1 and 2, pads 2 and 3, pads 3 and 4 and pads 4 and 1, respectively.[42] Copyright 2023, Elsevier.

Open Access Article. Published on 16 September 2024. Downloaded on 2/10/2026 6:27:48 AM.
This article is licensed under a Creative Commons Attribution-NonCommercial 3.0 Unported Licence.

developed soft candy-sensor *via* multiplexed measurements holds great promise for the POC testing of salivary electrical conductivity. However, conductometric biosensors generally have lower sensitivity and selectivity compared to other electrochemical biosensors, and the response can be affected by the ionic strength of the sample.

Electrochemical biosensors offer a versatile and powerful platform for CKD detection. Their ability to provide rapid, sensitive, and quantitative results makes them suitable for both clinical and POC applications. How to facilitate the transfer of electrons between the electrode and the analyte is critical for the function of electrochemical biosensors. Hence, nanomaterials like carbon nanotubes, graphene, nanosheets and metal nanoparticles are used to enhance the sensitivity and selectivity of electrochemical biosensors by providing a larger surface area and better electron transfer rates.[34] Besides, the diagnosis of CKD usually requires the simultaneous diagnosis of multiple indicators. The development of multiplexed voltammetric and amperometric biosensors that can simultaneously detect multiple CKD biomarkers improves diagnostic accuracy and efficiency.[37,41] Moreover, the integration of electrochemical biosensors into wearable devices for continuous monitoring of CKD biomarkers enables real-time health monitoring.[40]

2.2 Fluorescent biosensors

Fluorescent biosensors are a powerful and sensitive tool for the detection and monitoring of biomarkers associated with CKD. The high sensitivity, specificity, and ability to provide real-time data make these biosensors invaluable tools in CKD diagnostics.[44] Fluorescent biosensors can be classified into two categories, which are the "turn-on" and "turn-off" strategies. In the "turn-on" strategy, the signal generation mechanism ensures that fluorescence only occurs when the target is present, making these sensors highly sensitive and specific. In the "turn-off" strategy, the fluorescent biosensor emits a signal in the absence of the target, while the signal decreases or is quenched upon binding to the target. In this section, recent fluorescent biosensors for the detection of CKD biomarkers are summarized.

2.2.1 "Turn-on" fluorescent biosensors. "Turn-on" fluorescent biosensors are powerful tools for sensitive and

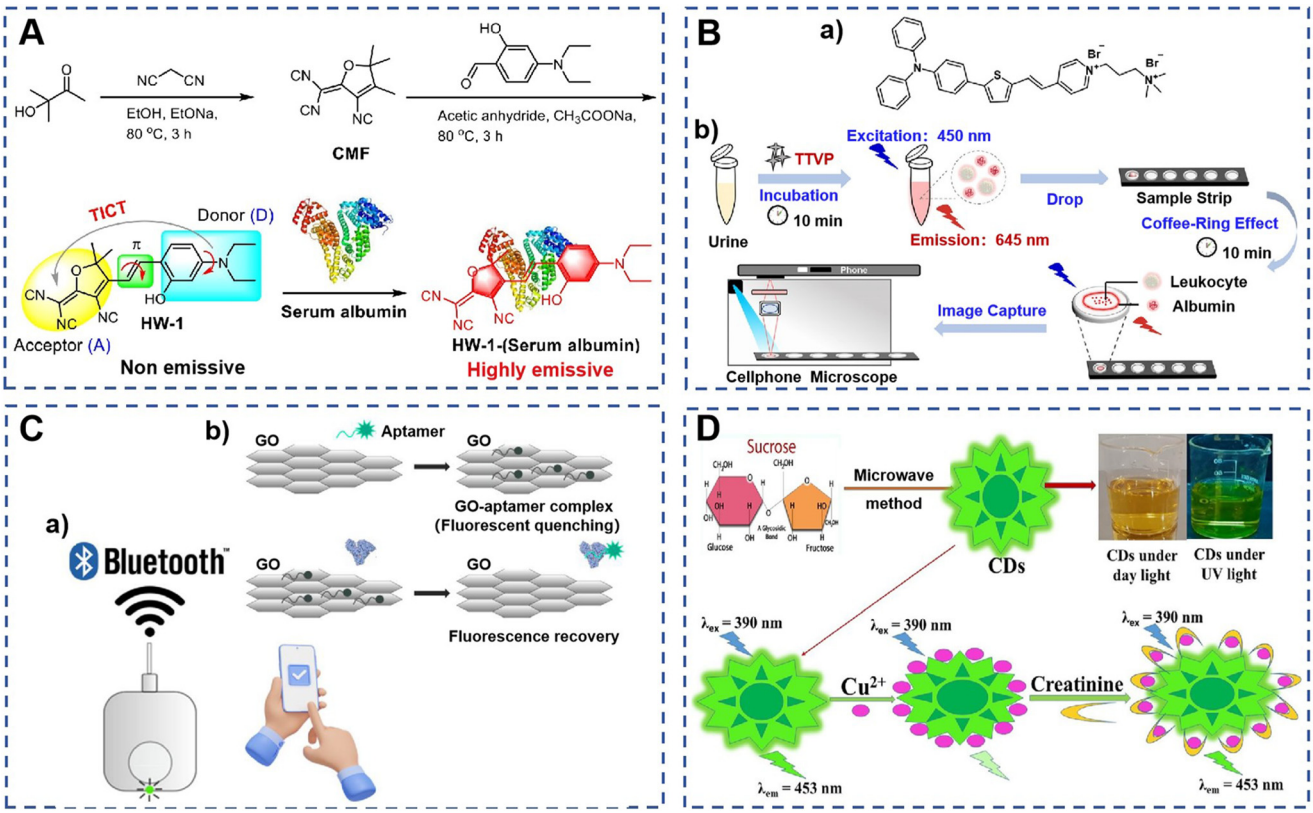

Fig. 5 Schematic illustration of "turn-on" fluorescent biosensors for detection of CKD biomarkers. (A) The synthesis of probe HW-1 and the mechanism for the "turn-on" fluorescence signal generated upon the interaction of probe HW-1 with serum albumin.[46] Copyright 2023, Elsevier. (B) Chemical structure of TTVP (a); schematic assay protocol and detection setup for the simultaneous quantification of albumin and leukocytes in one drop of urine (b).[47] Copyright 2022, American Chemical Society. (C) Schematic of the fluorometer with an integrated graphene oxide (GO)–aptamer biosensor and a custom smartphone device for the detection of HSA. (a) The fluorometer is combined with the smartphone application. (b) An illustration of the GO–aptamer assay principle demonstrates that the fluorescence signal is absent when fluorescence-labeled aptamers bind to GO, resulting in fluorescence quenching. In the presence of the target molecules, the aptamers bind to them, dissociating from GO and leading to the recovery of the fluorescence signal.[48] Reproduced with permission (Pinrod *et al.*, 2023 (ref. 48)). (D) Scheme depicting the synthesis of carbon dots as well as the illustration of a carbon dot-based biosensor for the detection of creatinine.[49] Copyright 2023, Elsevier.

© 2024 The Author(s). Published by the Royal Society of Chemistry

Open Access Article. Published on 16 September 2024. Downloaded on 2/10/2026 6:27:48 AM. This article is licensed under a Creative Commons Attribution-NonCommercial 3.0 Unported Licence.

specific detection of target molecules in various applications, since an increase in fluorescence provides a clear and unambiguous indication of the presence of the target analyte, making these biosensors more straightforward to use and interpret.[45]

One kind of fluorescent probe is a small-molecule, "turn-on" fluorescent biosensor often based on the intramolecular charge transfer (ICT) mechanism. Briefly, the fluorescence probe shows a weaker signal because of the ICT effect, while in the presence of the target, the fluorescence probe binds to the target, leading to suppression of non-radiative energy loss pathways, thereby enhancing fluorescence. For instance, Wang *et al.* synthesized a long wavelength turn on fluorescent probe HW-1 with a large Stokes shift (Fig. 5A).[46] In the absence of serum albumin, the fluorescence signal of probe HW-1 is weakened due to the twisted ICT (TICT) effect. In the presence of serum albumin, the HW-1 probe binds to serum albumin, suppressing non-radiative energy loss pathways and restoring fluorescence intensity. The designed HW-1 fluorescent probe is simple, has lower interference from auto-fluorescence, and can be used for the quantitative detection of serum albumin in complex samples. Therefore, the developed biosensor is an ideal tool for CKD diagnosis.[46] Besides, luminogen molecules with aggregation-induced emission (AIEgens) properties are also used to establish fluorescent biosensors. As a paradigm, Guan *et al.* designed a rapid turn-on fluorescent biosensor for the simultaneous quantification of human serum albumin (HSA) and leukocytes using an AIEgen molecule TTVP probe (Fig. 5B). In the presence of HSA, the TTVP probe shows high specificity to the hydrophobic pocket of HSA. Once interaction happens between TTVP and HSA, the non-radiative pathways were suppressed and then the luminogen becomes luminescent due to the restriction of intramolecular motion, leading to a significant fluorescence enhancement.[47] Interestingly, this well-designed biosensor only took 20 min for urine samples based on a smartphone-based detection device with a LOD of 18.75 mg L^{-1} for HAS, which provides a rapid, convenient and low-cost method for on-site urinary analysis.

Besides, the "turn-on" strategy can also be based on the fluorescence resonance energy transfer (FRET) mechanism. Briefly, the transfer occurs when the donor fluorophore, excited by an external light source, transfers its energy to the nearby acceptor fluorophore through dipole–dipole interactions. As a paradigm, Pinrod *et al.* developed an aptamer-based biosensor for the quantitative detection of HSA in urine samples. In this aptasensor, the aptamer labeled with Cy5 was used as a signal probe as well as a recognition probe, and graphene oxide (GO) was used as the fluorescence quencher. The single-stranded aptamer combined with GO leads to fluorescence quenching; in the presence of HSA, the aptamer binds to HSA and is hence released from the GO, restoring fluorescence intensity (Fig. 5C). The simple designed biosensor showed high sensitivity and selectivity for HSA detection, with a relatively low detection limit of 0.203 μg mL^{-1}. Moreover, the biosensor used a portable fluorometer to collect signals and has great potential in POC tests.[48]

Besides, nanomaterials (NMs) such as carbon-based NMs, quantum dots (QDs), metal-based NMs, metal–organic frameworks (MOFs), and upconversion NMs are also used to fabricate fluorescent biosensors owing to their tunable surface characteristics and unique optical and luminescence spectra. As a paradigm, a highly luminescent carbon dot (CD) based fluorescent "turn-on" biosensor was developed to detect creatinine (CR) in urine samples. The fluorescence of CDs with plentiful COO^- and OH^- groups could be easily quenched by Cu^{2+} ions. In the presence of CR, the empty d-orbitals of Cu^{2+} atoms are drawn to the lone pair of the N-atoms of CR. The electrostatic attraction between Cu^{2+} atoms and CR can cause the adsorption of the Cu^{2+} ions on the surface of CDs to decrease, thus the fluorescence intensity of CDs is recovered (Fig. 5D). Compared with previous methods, this developed biosensor exhibited better behavior, which was able to maintain a linear range from 10^{-5} to 0.1 mg dL^{-1} and a detection limit of 5.1×10^{-16} mg dL^{-1}.[49] How to select the most suitable fluorescence NMs depends on many factors, such as analyte concentration and its chemical nature. Recently, Bhatt *et al.* published a review focused on the performance evaluation of fluorescent NMs for CKD biomarkers across different types of fluorescent NMs. The advantages and disadvantages of fluorescent NMs were also discussed in detail to help gain a better knowledge on the sensing potential against CKD biomarkers.[50]

2.2.2 "Turn-off" fluorescent biosensors. In contrast to "turn-on" fluorescent biosensors, the fluorescence signal decreases or is quenched upon binding to the target in "turn-off" fluorescent biosensors. The fluorescence intensity is inversely proportional to the target concentration. For example, Pérez-Márquez *et al.* developed a novel turn-off fluorescent biosensor for selective detection of 3-nitrotyrosine in human blood serum based on the tetraphenylethene (TPE) molecular cage (Fig. 6A). This sensor was designed using a typical aggregation-induced emission material TPE to bind to 3-nitrotyrosine. Such supramolecular interaction concomitantly induces fluorescence quenching due to an electron transfer towards the electron-poor aromatic compound. After optimization, the fluorescent biosensor showed satisfactory results for the detection of 3-nitrotyrosine in serum samples, and the limit of detection in diluted mixture was 23 μM.[51] In another study, Thammajinno *et al.* fabricated a glutathione-capped copper nanocluster (GSH-CuNC) fluorescent biosensor for the detection of dual targets, human serum albumin (HSA) and creatinine, in human urine.[52] In this biosensor, the detection of creatinine was in a "turn-off" mode *via* non-covalent bonding under acidic conditions while the detection of HSA was in a "turn-on" mode *via* electrostatic interaction under basic conditions. Under optimal conditions, the developed nanocluster probe showed a fast response to the targets with the linear range

Open Access Article. Published on 16 September 2024. Downloaded on 2/10/2026 6:27:48 AM.
This article is licensed under a Creative Commons Attribution-NonCommercial 3.0 Unported Licence.

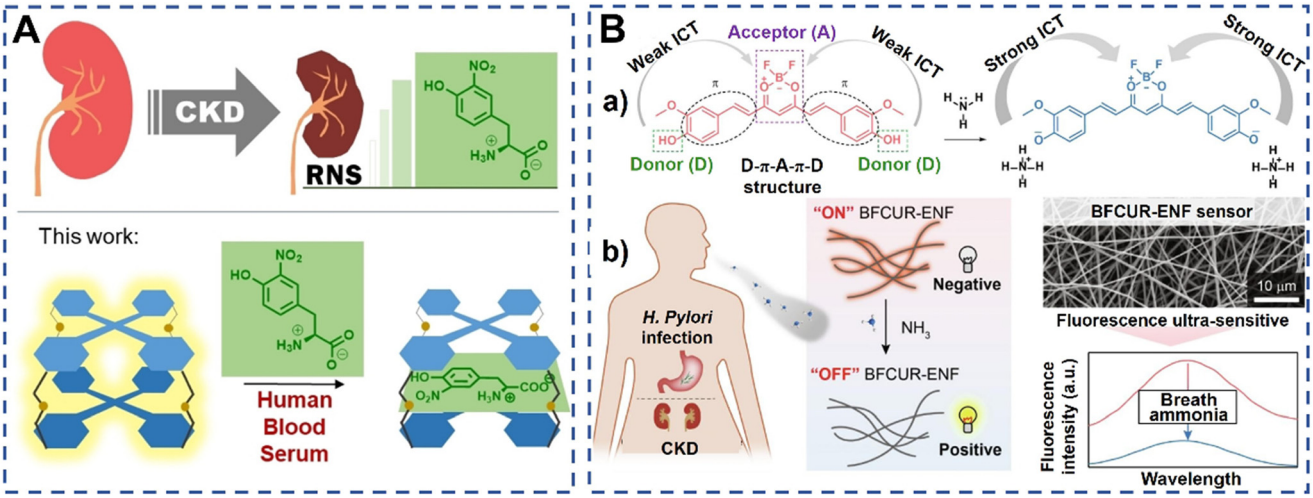

Fig. 6 Schematic illustration of "turn-off" fluorescent biosensors for detection of CKD biomarkers. (A) The developed supramolecular sensor of 3-nitrotyrosine (NT): a tetraphenylethene molecular cage turn-off sensor that works in human blood serum, since CKD could increase NT in blood due to nitration of tyrosine by reactive nitrogen species (RNS).[51] Copyright 2022, Wiley. (B) Schematic illustration of breath ammonia fluorescent sensor BFCUR-ENF based on the ICT effect (a) and the application in CKD or *Helicobacter pylori* (*H. pylori*)-infected patients (b).[53] Copyright 2022, Elsevier.

and detection limit of creatinine being 30 μM to 1000 μM and 13.0 μM, while those of HSA were 5.0 nM to 150 nM and 1.51 nM.

Based on the ICT effect, Song *et al.* rationally designed a "turn-off" fluorescent biosensor using curcumin (CUR) as the recognition probe for the detection of ammonia (Fig. 6B). Briefly, CUR also as the parent fluorophore has strong intermolecular π–π stacking which makes it unable to emit solid-state fluorescence due to the aggregation fluorescence quenching effect, thus boron trifluoride (BF) was introduced into CUR molecules to form a D–π–A–π–D conjugated system. ICT interactions occurred in the presence of ammonia, and an improved sensitivity was obtained due to the two binding sites of BFCUR. Besides, BFCUR was loaded into electrospun nanofibers (ENFs) with high specific surface area, which further improved the detection sensitivity. Finally, the obtained biosensor showed excellent performance in breath ammonia detection with an ultra-low LOD of 22 ppb.[53]

In summary, fluorescent biosensors have many advantages, such as: capability to detect very low levels of CKD biomarkers with high precision, making them ideal for early-stage detection; capability to simultaneously detect multiple biomarkers by using different fluorophores, providing a more comprehensive analysis; real-time monitoring of biomarker levels, which is valuable for dynamic studies and ongoing patient management. The drawbacks are summarized as follows: they require complex instrumentation (*e.g.*, spectrophotometers, lasers) and expensive reagents (fluorophores), which can limit their practicality in resource-limited settings; the fluorophores can degrade over time (photobleaching), leading to a decrease in signal intensity and potential loss of data accuracy; they suffer from high background noise due to autofluorescence from biological samples, complicating the interpretation of results.

Compared with the "turn-on" strategy, the "turn-off" strategy has been less reported mainly for the following reasons: (1) the signal-to-noise ratio in "turn-off" biosensors may be lower than in "turn-on" sensors, as the decrease in fluorescence can be subtle and easily masked by noise, making detection less reliable; (2) factors such as photobleaching can further complicate the measurement of the signal decrease; (3) "turn-off" biosensors may have a limited dynamic range, as they rely on a decrease in signal which can only go down to zero. This can restrict the range of concentrations that can be effectively measured; (4) designing effective "turn-off" fluorescent biosensors can be more complex, requiring careful selection and engineering of the fluorophore and quencher to ensure a significant and specific response to the target analyte. Considering these drawbacks, researchers often prefer "turn-on" biosensors or develop strategies to mitigate these challenges when working with "turn-off" fluorescent biosensors.

2.3 Colorimetric biosensors

Colorimetric biosensors are promising due to their rapid detection capabilities and potential for POC applications in clinical settings.[54] Since the color change can be observed visually or measured using simple optical instruments, colorimetric biosensors are suitable for rapid and easy-to-use detection in various applications, including medical diagnostics, environmental monitoring, food safety, and drug discovery.[55] In this section, recent colorimetric biosensors for the detection of CKD biomarkers are summarized.

Anthocyanins, pH-responsive flavonoid dyes, are often used to establish a colorimetric biosensor, owing to their

© 2024 The Author(s). Published by the Royal Society of Chemistry

Open Access Article. Published on 16 September 2024. Downloaded on 2/10/2026 6:27:48 AM. This article is licensed under a Creative Commons Attribution-NonCommercial 3.0 Unported Licence.

high water-solubility and good capability to display different colorimetric shades at different pH values. For example, Al-Qahtani *et al.* reported a simple, sustainable, reversible and cheap viscose (Vis) fabric colorimetric biosensor for sensitive detection of urea. In this biosensor, natural anthocyanin (Ac) was used as a spectroscopic probe and urease enzyme was used as a catalyst. In the presence of urea, the Ac probe embedded in calcium alginate could display ratiometric variations in the absorption spectra with the increase of concentration of urea in aqueous medium. Under optimal conditions, the developed biosensor sensitively detects urea with a linear range of 300–1000 ppm.[56] Moreover, Passornraprasit *et al.* developed a novel GO/CNF/PAA nanocomposite hydrogel sensing platform for colorimetric and LDI-MS determination of urea in sweat. This colorimetric biosensor was based on the enzymatic reaction catalyzed by urease with the chromogenic reaction of phenol red. The sensing reagents and enzymes were stored in the hydrogel with high water-sorption capacity and transparency properties. The mechanical properties and polymer functionalities of the hydrogel were improved by cellulose nanofibers (CNFs) and GO. Thus, the non-invasive and sensitive hydrogel-based biosensor was designed for urea detection with a vibrant distinguished color perception range from 40 to 80 mM.[57] In order to achieve dual detection, Chi *et al.* developed a biodegradable fluidic device using a hydrogel-based sensing platform for the colorimetric detection of glucose and creatinine in saliva samples. The cost-effective device consists of two parts: a sample collection part and a sensing module containing enzymes and dyes, which is easy to use for patients. Besides, the developed sensor could quantitatively detect biomarkers in saliva both spectrophotometrically and by smartphone-based analysis, showing its potential in POC diagnostics (Fig. 7A).[58]

Nanomaterials with peroxidase-like activity are often more stable than natural enzymes under extreme conditions of pH, temperature, and ionic strength. Besides, the catalytic activity of NMs can be tuned by controlling their size, shape, composition, and surface modifications. Hence, NMs have garnered significant interest in biosensing and medical diagnostics. As a paradigm, Nishan *et al.* developed a silver-doped activated carbon NP-based colorimetric biosensor for the detection of uric acid in human blood serum samples (Fig. 7B). In this biosensor, the NP complex was functionalized with 1-*H*-3 methyl imidazolium acetate ionic liquid to form the sensing platform. The chromogenic substrate 3,3′,5,5′-tetramethylbenzidine (TMB) was used with the support of H_2O_2. The mimic enzyme with the assistance of hydrogen peroxide converts the colorless TMB solution to a blue-green color. The addition of uric acid to the above

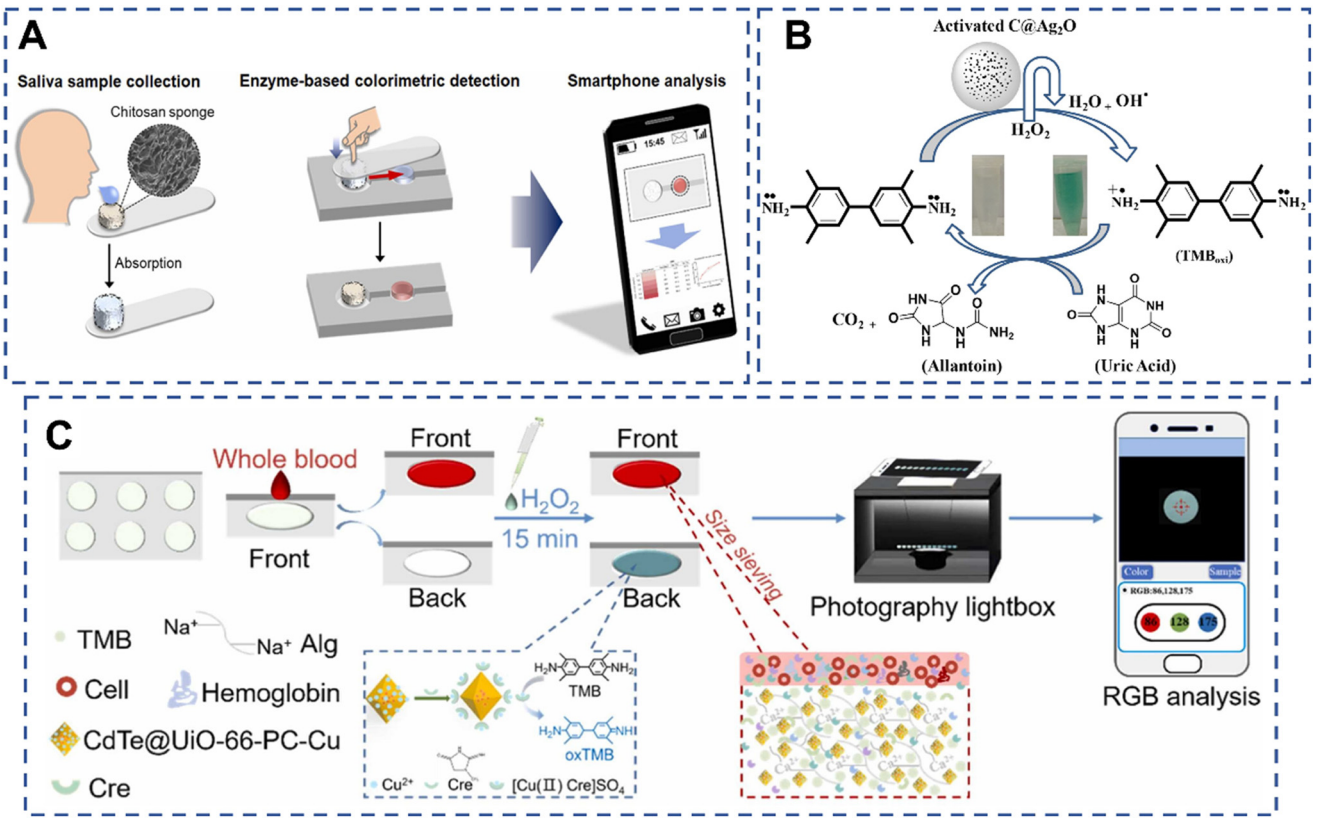

Fig. 7 Schematic illustration of colorimetric biosensors for detection of CKD biomarkers. (A) Schematic diagram of the overall process of the proposed saliva-based biosensing system.[58] Copyright 2023, Elsevier. (B) Ionic liquid capped Ag_2O/activated carbon NPs as a sensing platform for uric acid.[59] Copyright 2024, The Royal Society of Chemistry. (C) Schematic diagram of the mechanism and procedure of the hydrogel-based colorimetric paper analytical device platform for the Cre assay in human whole blood.[60] Copyright 2024, Elsevier.

Open Access Article. Published on 16 September 2024. Downloaded on 2/10/2026 6:27:48 AM. This article is licensed under a Creative Commons Attribution-NonCommercial 3.0 Unported Licence.

mixture resulted in the reduction of oxidized TMB to the reduced form with the change of color. Under optimal conditions, the biosensor was then demonstrated to be highly selective and sensitive for detection of uric acid in the concentration range from 0.001 to 0.36 μM and a low detection limit of 0.207 nM. Notably, the quantification detection capability of this biosensor was estimated to be as low as 0.69 nM, holding great potential for practical applications.[59] Moreover, Guan *et al.* constructed a novel functionalized CdTe@MOF based biosensor for the fluorometric and colorimetric dual-readout of creatinine (Cre) in human serum (Fig. 7C). In the colorimetric assay, similarly, H_2O_2 and TMB were chosen as substrates. In the presence of Cre, the CdTe@UiO-66-PC-Cu-Cre catalytic system displayed a strong absorption peak with the solution turning dark blue as observed by the naked eye, owing to the formed Cu^{2+}/Cre complex exhibiting a certain peroxidase activity that converts colorless TMB to blue oxTMB. Besides, a hydrogel-based c-PAD and smartphone-integrated portable platform was further designed for non-separation *in situ* visible determination of Cre in whole blood with a LOD of 1.78 μM,[60] holding great potential in CKD small molecule biomarker detection.

Colorimetric biosensors are ideal for POC and home testing and have the advantage of initial screening since this kind of biosensor requires no complex instrumentation, is inexpensive to produce and use, and provides rapid results typically obtained within minutes, besides, the results can be visually assessed. However, the sensitivity of colorimetric biosensors is generally less than that of electrochemical and fluorescent biosensors, making them less effective for detecting low concentrations of biomarkers. The color change is often subjective, making it challenging to quantify results accurately without the aid of additional devices like spectrophotometers. Additionally, colorimetric biosensors are susceptible to interference caused by sample color or turbidity and can be unstable under different environmental conditions (*e.g.*, temperature, pH).

Each biosensor type has its strengths and limitations in the context of CKD detection. The choice of biosensor should be guided by the specific application requirements, such as sensitivity, cost, and the testing environment. For example, fluorescent biosensors generally offer the highest sensitivity, followed by electrochemical biosensors, with colorimetric biosensors being the least sensitive; colorimetric biosensors are the simplest and most cost-effective but lack precision, while fluorescent sensors are highly sensitive but complex and expensive; electrochemical biosensors offer a balance, with good sensitivity and relatively low cost, but require careful design to minimize interference; both electrochemical and colorimetric biosensors are more suited for POC and low-resource settings due to their portability and ease of use. In contrast, fluorescent biosensors are better suited for laboratory settings where high sensitivity and multiplexing are required.

Although the above three categories of POC biosensors have made great progress, there are still some challenges to face: (1) the accuracy and reliability. Variability in biosensor performance, particularly in different patient populations, remains a concern. (2) Detection of early-stage CKD. Many POC biosensors still struggle to detect early-stage CKD accurately, particularly when biomarker levels are only slightly elevated. (3) Limitation to specific biomarkers and lack of comprehensive kidney function evaluation. (4) Gaining regulatory approval and clinical validation for new POC biosensors, particularly in terms of demonstrating their effectiveness in real-world settings.

In short, various biosensor-based methods used for diagnostic CKD in urine, serum, sweat, saliva and gas were summarized. The details of these biosensors are shown in Table 2.

3. POC devices for CKD detection

POC devices for CKD diagnostics offer a promising approach to improving the management and outcomes of CKD. By providing timely, accurate, and accessible testing, these devices enable better patient care, early intervention, and efficient disease monitoring.[62] Herein, the common POC devices and technologies used in CKD diagnostics, such as lateral flow devices, microfluidic-based analytical devices and lab-on-a-chip devices are summarized.

3.1 Lateral flow devices

Lateral flow (LF) devices are a powerful tool for CKD diagnostics, offering a rapid, cost-effective, and user-friendly solution for detecting key biomarkers. Their portability and ease of use make them particularly valuable for POC testing, enabling early detection and continuous monitoring of CKD. A typical LF device consists of four parts: a sample pad for sample fluid loading; a conjugate pad for storing bio-labels; a nitrocellulose (NC) membrane for testing; an absorbent pad for collecting excess sample fluid.

Most LF devices use antibodies as recognition materials, thus a large number of LF immunoassays were developed. For instance, Chotithammakul *et al.* designed a colorimetric LF assay for albumin detection. Anti-bovine serum albumin (anti-BSA) was modified on AuNPs, which were sprayed on a conjugate pad. In the presence of BSA, the AuNP@anti-BSA conjugates capture the BSA, thus the test line obtained a positive signal, and the signal intensity of the test line increased with an increase in the BSA concentration. This colorimetric lateral flow could effectively detect BSA with a concentration of 0.2 mg mL^{-1}, and the strong signal obtained reached 4 mg mL^{-1}.[63] Similarly, Natarajan *et al.* fabricated a fluorometric LF immunoassay for cystatin-C detection. Cystatin-C could bind to the AF647–cystatin-C conjugates and form a sandwich structure in the test line. Thus, a positive signal was obtained. After optimization, the LF immunoassay showed a linear range of 0.023–32 μg mL^{-1} with a lower LOD of

© 2024 The Author(s). Published by the Royal Society of Chemistry

Open Access Article. Published on 16 September 2024. Downloaded on 2/10/2026 6:27:48 AM. This article is licensed under a Creative Commons Attribution-NonCommercial 3.0 Unported Licence.

Table 2 Comparison table of developed biosensors for diagnosis of chronic kidney disease

Sensing type	Target	Sample	Linear range	LOD	Ref.
Voltammetric	Creatinine	Saliva	10–160 μM	0.1 μM	3
Voltammetric	Creatinine	Saliva	3.25–200 μM	1.3 μM	25
Voltammetric	Creatinine	Urine	0–8 mM and 8–18 mM	60 μM	26
Voltammetric	Ammonium ions	Urine	0.5–20 mM	290.1 μM	28
	Urea		0.5–15 mM	500 μM	
	Creatinine		2–16 mM	562.5 μM	
Voltammetric	Albumin	Urine	—	0.09 nM	29
Voltammetric	Cystatin C	Serum	0.1–1000 ng mL^{-1}	33 pg mL^{-1}	30
Voltammetric	Creatinine	Saliva	5–30 μM	90 nM	31
Voltammetric	Albumin	Urine	5.0–100 ng mL^{-1}	1.5 ng mL^{-1}	32
	Creatinine		5.0–100 and 100–2500 ng mL^{-1}		
Voltammetric	Creatinine	Serum and saliva	200–1000 nM	340 pM	33
Voltammetric	Creatinine	Urine	10^{0}–10^{12} fg ml^{-1}	0.27 fg mL^{-1}	34
	Urea	Serum and saliva	10^{2}–10^{12} fg ml^{-1}	3.87 fg mL^{-1}	
	HSA	Serum and saliva	10^{0}–10^{8} fg ml^{-1}	0.52 fg mL^{-1}	
Amperometric	Ammonia	Gas	300–2000 ppb	—	36
Amperometric	Ammonia	Gas	400 ppb–20 ppm	400 ppb	37
Amperometric	Ammonia	Gas	0.4–3 ppm	0.4 ppm	38
Amperometric	Urea		0.01–1 mM	3.56 μM	39
Amperometric	Urea	Sweat	0–100 mM	20 mM	40
Amperometric	Glucose	Serum	0.5–18 mM	6.02 μM	41
	Creatinine		0.04–1 mM	1.95 μM	
	Uric acid		0.04–0.8 mM	3.1 μM	
Amperometric	Phosphate	ISF	0.3–1.8 mM	0.1 mM	61
	Uric acid		50–550 μM	31 μM	
	Creatinine		50–550 μM	18 μM	
	Urea		1–16 mM	0.49 mM	
Conductometric	—	Saliva	—	0.01 M (206 μS cm^{-1})	42
Conductometric	—	Saliva	—	1630 μS cm^{-1}	43
Fluorescent	HSA	Serum	0–40 μM	54 nM	44
Fluorescent	HSA	Urine	18.75–300 mg L^{-1}	18.75 mg L^{-1}	47
	Leukocytes		25–400 mg μL^{-1}	—	
Fluorescent	HSA	Serum	0.001–1.5 mg mL^{-1}	0.203 μg mL^{-1}	48
Fluorescent	Creatinine	Urine	10^{-5}–0.1 mg dL^{-1}	5.0×10^{-6} mg dL^{-1}	49
Fluorescent	3-Nitrotyrosine	Serum	—	16 μM	51
Fluorescent	Creatinine	Urine	30–1000 μM	1.510 nM	52
	HSA		5.0–150 nM	13 μM	
Fluorescent	Ammonia	Gas	0–10^{4} ppb	22 ppb	53
Fluorescent	Creatinine	Blood	0–400 μM	2.48 nM	60
Fluorescent	Indophenol sulfate	Serum and urine	10^{-5}–5×10^{-3} M	1.4 μM	62
	Indophenol sulfate		10^{-5}–5×10^{-2} M	1.6 μM	
Colorimetric	Urea	Urine	0–500 mM	0.58 mM	12
Colorimetric	Urea	Saliva	50×10^{-3}–1 M	—	54
Colorimetric	Urea	Blood and urine	300–1000 ppm	0.0031 ng mL^{-1}	56
Colorimetric	Urea	Sweat	40–80 mM	60 mM	57
Colorimetric	Glucose and creatinine	Saliva	—	20.444 ng mL^{-1}	58
Colorimetric	Uric acid	Serum	0.001–0.36 μM	0.2 pg mL^{-1}	59
Colorimetric	Creatinine	Blood	0–600 μM	1.78 μM	60

0.023 μg mL^{-1}.[64] The LF based on fluorescence signals is usually more sensitive than that based on colorimetric signals, but both of them need 15 min for detection.

Besides, colorimetric LF assays using enzymatic reactions are a type of POC diagnostic tool that combines the simplicity of lateral flow technology with the sensitivity and specificity of enzymatic colorimetric detection. As a paradigm, Cheng *et al.* designed a paper-based colorimetric biosensor for blood urea nitrogen (BUN) detection. In this device, the test strip contains multi-layered films (mesh, blood separation membrane, filter film, reaction film) to store reagents and enzymes. It is slightly different from traditional LF devices; the sample injection hole is also used as a colorimetric area in this device (Fig. 8). Under optimal conditions, the designed test strip can quickly detect BUC in blood samples within 2 min, and with a low detection limit of 0.03 mM, demonstrating its great potential for POC applications.[65]

3.2 Microfluidic-based analytical devices

Microfluidic-based analytical devices for CKD leverage the precision and efficiency of microfluidics technology to provide rapid, accurate, and cost-effective diagnostics that

Open Access Article. Published on 16 September 2024. Downloaded on 2/10/2026 6:27:48 AM.
This article is licensed under a Creative Commons Attribution-NonCommercial 3.0 Unported Licence.

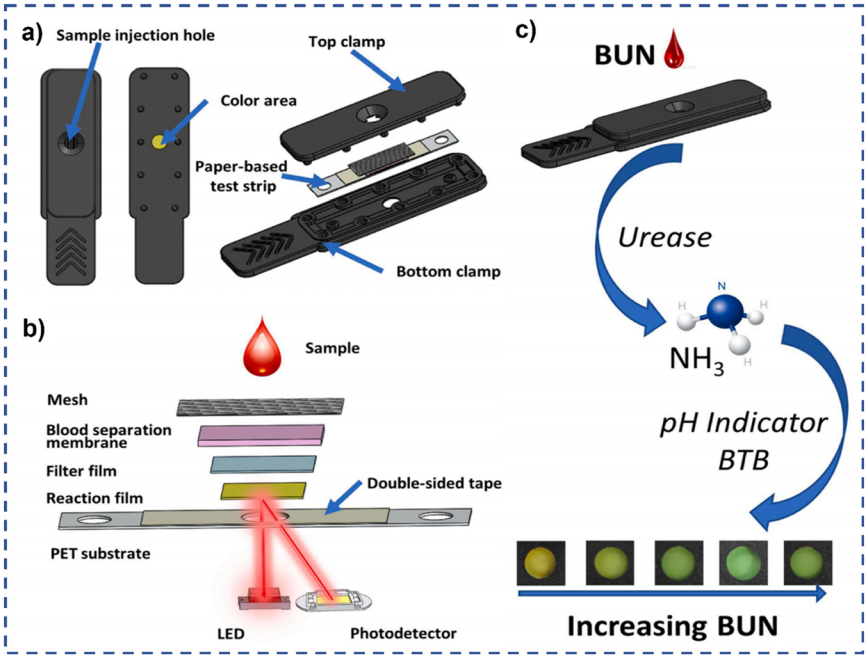

Fig. 8 (a) Schematic diagram of a disposable photochemical test strip; (b) the composition of the multilayer film strip and a schematic diagram of reflectance photometry; (c) the principle of the enzymatic colorimetric reaction.[65] Copyright 2023, Elsevier.

are essential for early detection, regular monitoring, and effective management of CKD.[66] These devices integrate multiple laboratory functions into a single, compact chip, allowing for the detection and monitoring of biomarkers relevant to CKD with minimal sample volumes of fluids through microchannels.[67] As technology continues to evolve, microfluidic devices will become even more integral to personalized healthcare and precision medicine.

For example, Tseng *et al.* developed a microfluidic aptasensor POC device for detection of whole blood potassium.[68] The designed microfluidic device comprises two main parts, an AuNP aptasensor PMMA/paper-microchip and a colorimetric analysis system. In this system, the AuNPs in the AuNP/aptamer complex are displaced by the serum K^+ ions and react with NaCl to produce a color change in the detection region from which the K^+ ion concentration is then inversely derived. Briefly, in performing the microfluidic detection process, the PMMA/paper-microchip was switched to the reagent mode, thus a finger pump (F1) was then used to deliver reagent B (aptamer) to the detection zone. After waiting for the aptamer to bind with AuNPs, the excess aptamer will flow into the waste chamber. Then the whole blood sample was injected to the sample chamber, and the PMMA/paper-microchip was switched to the reaction mode. Later, a second finger pump (F2) was activated to drive reagent C (NaCl) to the detection zone to facilitate a colorimetric reaction (Fig. 9). This handheld microfluidic device provides a linear response over the K^+ ion concentration in the range of 0.05–9 mM in artificial serum and has a detection limit of 0.01 mM, with a price of less than 0.5 dollar per microchip.[68] Besides, Ferrira *et al.* designed an on-hand microfluidic paper-based device for ammonium and urea determination in saliva. In this analytical device, the NH_x detection was based on the conversion of ammonium to ammonia, followed by its diffusion through a hydrophobic membrane and then the color change of a bromothymol blue (BTB) indicator, while in the urea detection, prior to the ammonium conversion and BTB color change, the enzymatic conversion of urea into ammonium was produced, using urease. Under optimal conditions, the microfluidic paper-based device attained a quantification range of 0.1–5.0 mM and 0.16–5.0 mM with a

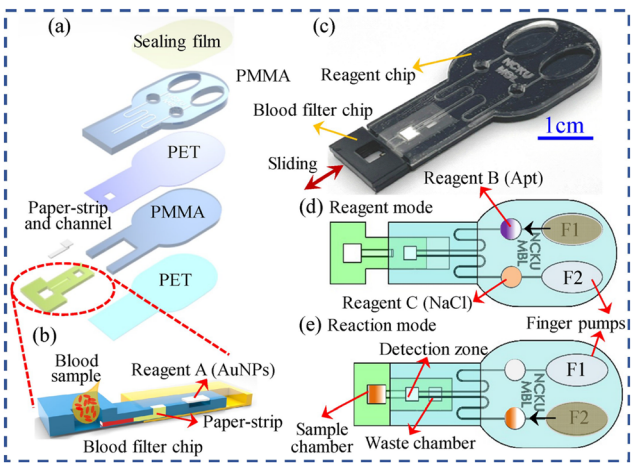

Fig. 9 Schematic illustration and photograph of the PMMA/paper-microchip. (a) The split diagram of the reagent chip and the whole blood filter chip; (b) the cross-sectional structure of the whole blood filter chip and the process of separating a whole blood sample into serum and transferring it to the reaction zone; (c) the combination diagram of the chip; (d) the reagent mode; (e) the reaction mode.[68] Copyright 2022, Elsevier.

© 2024 The Author(s). Published by the Royal Society of Chemistry

Open Access Article. Published on 16 September 2024. Downloaded on 2/10/2026 6:27:48 AM. This article is licensed under a Creative Commons Attribution-NonCommercial 3.0 Unported Licence.

detection limit of 0.032 mM and 0.049 mM for NH_x and urea, respectively.[69]

Sensor arrays can be assembled on a paper substrate in order to save cost and consumption of reactants, inject low sample volumes, reduce analysis time, and help run tests at the sampling site.[70] Hence, Bordbar *et al.* designed a sensor array-based microfluidic structure with 16 detection zones. This sensor consists of three parts: a large central circle for the sample injection, 16 small circles to immobilize the receptors, and the channels that connect the two parts. The detection zone was filled with different color compounds, including metal NPs and organic dyes. After optimization, this sensor array exhibited greater sensitivity than the standard methods. However, the performance of this sensor must be tested in the studies with a larger sample size, since the individual difference.[70]

3.3 Lab-on-a-chip devices

Lab-on-a-chip (LOC) devices are a subset of microfluidic devices aiming to miniaturize and automate laboratory processes, creating a portable, efficient, and often fully integrated platform for complex analyses, offering significant advantages for CKD diagnostics, including reduced sample volumes, enhanced sensitivity, and the ability to perform complex analyses in a compact, portable format.[71]

Continuous monitoring is essential for the early diagnosis of kidney disease, thus wearable devices offer a promising alternative to traditional laboratory tests by enabling rapid, on-site diagnosis and monitoring of CKD. As a paradigm, Zhang *et al.* designed a microneedle coupled epidermal electrochemical sensor array (MNESA) for multiplexed detection of kidney disease biomarkers. Four working electrodes were modified with specific enzymes to enable selective detection of their respective substrates, and then integrated into a small electrode patch with a reference electrode and a counter electrode (Fig. 10A). Through thumb pressure on the skin, the stratum corneum is penetrated, and interstitial fluid (ISF) containing biomarkers is rapidly extracted onto an electrochemical sensor array. Hence, the

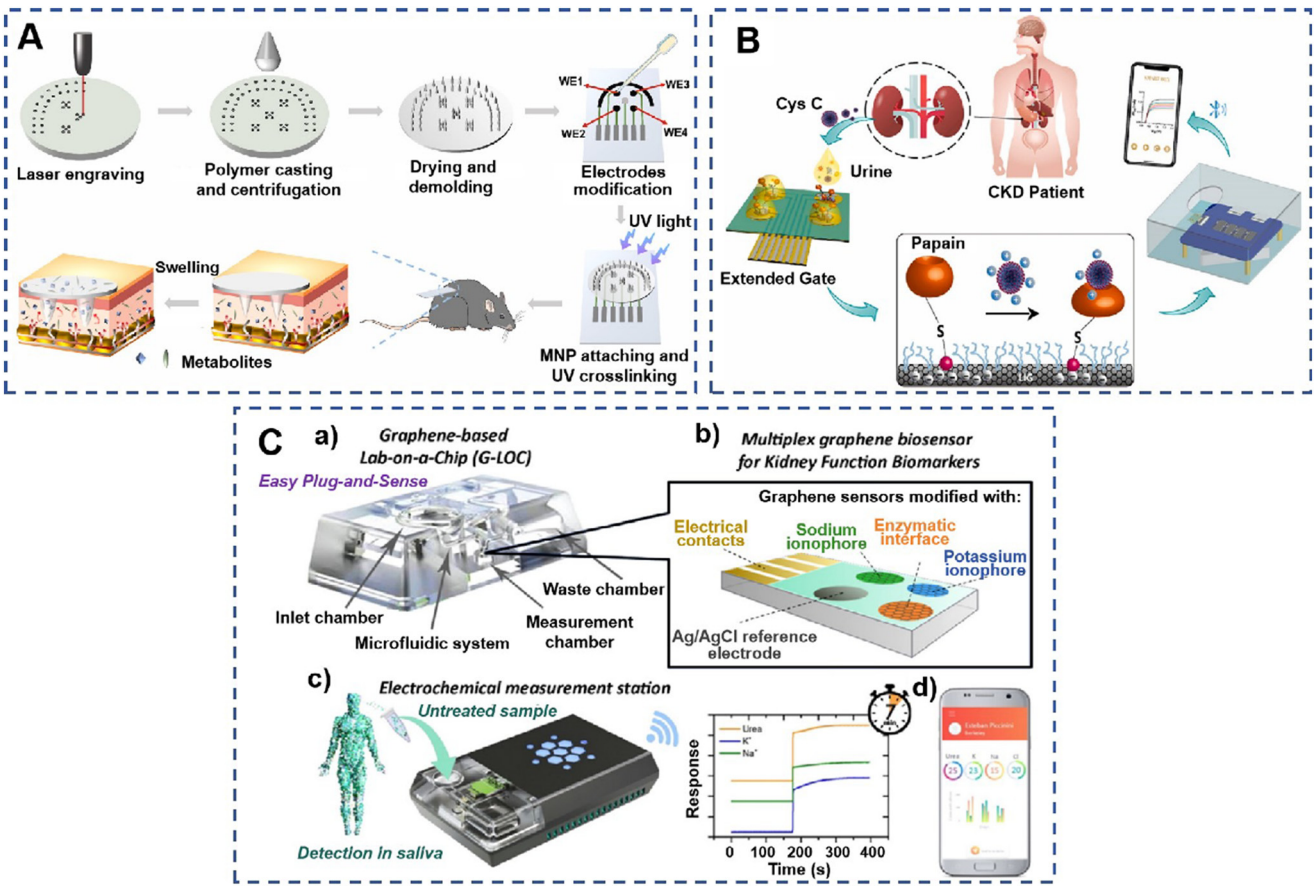

Fig. 10 Schematic illustration of LOC devices. (A) Schematic illustration of the fabrication process and application of MNESA.[61] Copyright 2023, Elsevier. (B) Schematic illustration of non-invasive detection of u-Cys C *via* the multilevel interface-engineered graphene EG-FET sensor.[72] Copyright 2024, Elsevier. (C) Schematic illustration of the microfluidic system description of the G-LOC for the detection of CKD biomarkers. (a) Microfluidic system description of the G-LOC. (b) Schematic representation of the multiplex biosensor for kidney function biomarkers. (c) Bioelectronics assay using saliva or serum. The G-LOC is connected to the electrochemical measurement station by an easy plug-and-sense manner. Simultaneous response was measured for each biomarker as a function of time during the test run. (d) Test results are displayed in software for mobile devices.[73] Copyright 2024, American Chemical Society.

Open Access Article. Published on 16 September 2024. Downloaded on 2/10/2026 6:27:48 AM. This article is licensed under a Creative Commons Attribution-NonCommercial 3.0 Unported Licence.

well-developed MNESA can achieve wearable and specific detection of phosphate, uric acid, urea, and creatinine in ISF of the skin with a physiologically relevant range, demonstrating an ideal POC device for commercial use.[61]

The lack of standardized protocols for wearable LOC devices can hinder widespread adoption and comparability of results. Besides, invasive LOC devices often have the shortcoming of the interference from other substances in the complex biological matrix of interstitial fluid. Hence, Chen *et al.* developed a non-invasive extended-gate field-effect transistor (EG-FET) sensor for urine cystatin (Cys) C detection (Fig. 10B). The sensor is capable of detecting low concentrations of analytes due to the high sensitivity of the FET to surface charge changes. The modification of NMs on electrodes could further enhance the electron transfer properties, in this case, AuNPs and laser-induced graphene (LIG) were used in the sensing platform. Hence, the highly integrated EG electrode sensing chip showed a wide detection range for Cys C detection with an extremely low detection limit of 0.05 ag μL^{-1}, demonstrating a new strategy for POC diagnostics. Besides, FET-based sensors generally require low power, making them suitable for battery-operated devices.[72] To increase the throughput and efficiency of testing, multiple analyses can be performed simultaneously on a single chip. As a paradigm, Diforti *et al.* designed a multiplex and non-invasive graphene-based LOC (G-LOC) device for self-testing of CKD biomarkers (Fig. 10C). The integrated sensing system always uses small sample volumes, and the modification of graphene on the electrode can ensure a rapid response during testing. The G-LOC was further integrated in a microfluidic cassette to connect to a portable electrochemical measurement station (Zaphyrus-W20). The Zaphyrus-W20 is intelligent and easy to use, and can connect to a smartphone or computer software to send reports, making the device highly promising for POC clinical diagnostics.[73]

In summary, POC technologies enable rapid, on-site diagnostic testing, offering numerous advantages over traditional methods. The growing interest in POC biosensors is driven by the need for more accessible and cost-effective diagnostic solutions, including primary care clinics, remote areas, and even patients' homes. LF devices are best suited for simple, rapid, and cost-effective CKD screening, particularly in low-resource or home settings. They are limited by lower sensitivity and quantification challenges but are highly accessible. Microfluidic-based analytical devices offer greater sensitivity, specificity, and the ability to perform multiplexed tests with minimal sample volume. But their complexity and cost may limit widespread use in resource-constrained environments. And LOC devices represent the pinnacle of integration and miniaturization, offering comprehensive, high-throughput diagnostic capabilities. They are ideal for POC and personalized monitoring but require sophisticated technology and manufacturing processes. The advantages and disadvantages of POC devices for CKD diagnostics are summarized in Table 3.

4. Conclusions and future perspectives

This review underscores significant advancements in CKD diagnostics, emphasizing the transformative impact of POC biosensors and devices. The advances in materials science, nanotechnology, and electronics are likely to further improve the performance and accessibility of POC biosensors,[54] making them an increasingly important tool in the diagnostics of CKD. Besides, POC devices enhance accessibility, particularly in remote or resource-limited settings, facilitating early detection and timely intervention, which are crucial for effective CKD management. Technological innovations, including LF,[65] microfluidics,[67] and LOC technologies,[71] offer rapid, accurate, and cost-effective diagnostic solutions, reducing reliance on extensive laboratory infrastructure. These devices target key biomarkers such as creatinine, albumin, cystatin C, HSA, urea and glucose, with multiplexing capabilities enhancing diagnostic accuracy. Moreover, the integration of POC devices with digital health platforms supports personalized medicine, enabling continuous monitoring, real-time data sharing, and tailored treatment plans, thereby improving patient compliance and engagement.[62]

However, several challenges must be addressed before these devices can be widely adopted in clinical practice. (1) POC devices may not always match the accuracy and precision of centralized laboratory testing, particularly for critical biomarkers like creatinine, cystatin C, or albumin. The inconsistent results can lead to misdiagnosis, inappropriate treatment, or failure to detect early-stage CKD.

Table 3 Comparisons of the POC devices for the diagnostics of chronic kidney diseases

Devices	Advantages	Disadvantages	Ref.
Lateral flow devices	Rapid results, ease of use, portability, low cost, independent of equipment or simple device, easy miniaturization and development	Limited sensitivity, limited quantitative detection, interference, limited multiple detection, storage requirements	63–65
Microfluidic-based analytical devices	Miniaturization, automation, high throughput, versatility, rapid, sensitive detection, accurate, low sample volumes and simple device	Complex fabrication, sample handling issues, integration challenges, limited standardization, user training	66–70
Lab-on-a-chip devices	Portable, efficient, high throughput, low sample volumes, integration of functions, good reproducibility and reliability	Complex fabrication, sample handling issues, standardization, user training	15, 61, 71–73

© 2024 The Author(s). Published by the Royal Society of Chemistry

Open Access Article. Published on 16 September 2024. Downloaded on 2/10/2026 6:27:48 AM. This article is licensed under a Creative Commons Attribution-NonCommercial 3.0 Unported Licence.

(2) Some POC devices may struggle with the sensitivity needed to detect low concentrations of biomarkers, which is crucial for early CKD detection. Additionally, LF devices can suffer from cross-reactivity with other substances in the sample, leading to false positives or inaccurate readings. (3) Microfluidic channels can become clogged or fouled by biological materials, particularly in samples like blood or urine that contain cells, proteins, and other particulates. Clogging can disrupt the assay, leading to inaccurate results or device failure, which is a significant challenge in ensuring consistent performance. (4) Both microfluidic and LOC devices have challenges in scaling up production, especially in resource-constrained settings, since microfluidic devices require precise fabrication techniques (*e.g.*, photolithography, soft lithography) and LOC devices need precise microfabrication techniques, such as etching, deposition, and bonding, which can be complex and costly.

While LF devices, microfluidic-based analytical devices, and LOC devices offer significant promise for CKD diagnosis, they face a range of technical, manufacturing, and operational challenges. Addressing these challenges will be key to realizing the full potential of these technologies in improving CKD diagnosis, particularly in point-of-care and resource-limited settings. Ongoing research and development efforts focused on enhancing sensitivity, reducing complexity, and improving scalability will be critical in overcoming these obstacles and expanding the accessibility and reliability of these diagnostic tools. Overall, POC biosensors and devices represent a paradigm shift in CKD diagnostics, promising improved patient outcomes and a reduction in the global burden of the disease through early detection, effective management, and personalized care strategies.

Data availability

No primary research results, software or code have been included and no new data were generated or analysed as part of this review.

Author contributions

Yuan Liu: conceptualization and writing – original draft, review and editing. Xinping Zhao: investigation and formal analysis; Min Liao: formal analysis; Guoliang Ke: project administration, funding acquisition, writing – review and editing and supervision. Xiao-Bing Zhang: resources, project administration, and supervision.

Conflicts of interest

The authors have no conflicts of interest to declare.

Acknowledgements

This work was supported by the National Natural Science Foundation of China (22122403, 62401248, 22234003).

References

1 S. L. Luo and T. M. Swager, *ACS Nano*, 2024, **18**, 364–372.
2 Divya, Darshna, A. Sammi and P. Chandra, *Biotechnol. Bioeng.*, 2023, **120**, 3116–3136.
3 A. Domínguez-Aragón, A. S. Conejo-Dávila, E. A. Zaragoza-Contreras and R. B. Dominguez, *Chemosensors*, 2023, **11**, 102.
4 K. V. Jarnda, D. Wang, Q. U. Ain, R. Anaman, V. E. Johnson, G. P. Roberts, P. S. Johnson, B. W. Jallawide, T. Kai and P. Ding, *Sens. Actuators, A*, 2023, **363**, 114778.
5 M. Salima, F. Rahmani and S. M. R. M. Hosseini, *Anal. Chem.*, 2021, **6**, 7829–7837.
6 M. Khokhar, *J. Breath Res.*, 2024, **18**, 024001.
7 P. P. Ricci and O. J. Gregory, *Sci. Rep.*, 2021, **11**, 7185.
8 S. Kose, R. E. Ahan, I. C. Koksaldi, A. Olgac, C. S. Kasapkara and U. O. S. Seker, *Biosens. Bioelectron.*, 2023, **223**, 115035.
9 D. Liang, Y. Wang and K. Qian, *Interdiscip. Med.*, 2023, **1**, e20230020.
10 Z. Dai, M. Lei, S. Ding, Q. Zhou, B. Ji, M. Wang and B. Zhou, *Exploration*, 2024, **4**, 20230046.
11 X. Gao, L. Feng, R. Deng, B. Wang, Y. He, L. Zhang, D. Luo, M. Chen and K. Chang, *Interdiscip. Med.*, 2024, **2**, e20230033.
12 C. K. Choi, S. M. Shaban, B. S. Moon, D. G. Pyun and D. H. Kim, *Anal. Chim. Acta*, 2021, **1170**, 338630.
13 F. Usman, K. H. Ghazali, R. Muda, J. O. Dennis, K. H. Ibnaouf, O. A. Aldaghri, A. Alsadig, N. H. Johari and R. Jose, *Chemosensors*, 2023, **11**, 119.
14 D. Kukkar, M. Chhillar and K. H. Kim, *Biosens. Bioelectron.*, 2023, **232**, 115311.
15 B. Karakuzu, E. A. Tarim, C. Oksuz and H. C. Tekin, *ACS Omega*, 2022, **7**, 25837–25843.
16 Y. Fu, Y. Liu, W. Song, D. Yang, W. Wu, J. Lin, X. Yang, J. Zeng, L. Rong, J. Xia, H. Lei, R. Yang, M. Zhang and Y. Liao, *Exploration*, 2023, **3**, 20230028.
17 A. Tricoli and G. Neri, *Sensors*, 2018, **18**, 942.
18 R. Bodington, X. Kassianides and S. Bhandari, *Clin. Kidney J.*, 2021, **14**, 2316–2331.
19 D. Kukkar, D. Zhang, B. H. Jeon and K. H. Kim, *TrAC, Trends Anal. Chem.*, 2022, **150**, 116570.
20 R. M. Gama, D. Nebres and K. Bramham, *Diagnostics*, 2024, **14**, 1542.
21 N. Yadav, J. Narang, A. K. Chhillar, J. S. Rana, M. U. M. Siddique, E. Kenawy, S. Alkahtani, M. N. Ahsan, A. K. Nayak and M. S. Hasnain, *Sens. Int.*, 2024, **5**, 100253.
22 P. J. Babu, A. Tirkey, T. J. M. Rao, N. B. Chanu, K. Lalchhandama and Y. D. Singh, *Anal. Biochem.*, 2022, **645**, 114622.
23 K. Sinha, Z. Uddin, H. I. Kawsar, S. Islam, M. J. Deen and M. M. R. Howlader, *TrAC, Trends Anal. Chem.*, 2023, **158**, 116861.
24 Y. Liu, T. Li, C. Ling, Z. Chen, Y. Deng and N. He, *Chin. Chem. Lett.*, 2019, **30**, 2211–2215.
25 S. Kumaravel, S. H. Wu, G. Z. Chen, S. T. Huang, C. M. Lin, Y. C. Lee and C. H. Chen, *Biosens. Bioelectron.*, 2021, **171**, 112720.

© 2024 The Author(s). Published by the Royal Society of Chemistry

Open Access Article. Published on 16 September 2024. Downloaded on 2/10/2026 6:27:48 AM. This article is licensed under a Creative Commons Attribution-NonCommercial 3.0 Unported Licence.

26 S. Bajpai, G. R. Akien and K. E. Toghill, *Electrochem. Commun.*, 2024, **158**, 107624.
27 M. Jagannathan, D. Dhinasekaran, A. R. Rajendran and S. Cho, *Biosensors*, 2023, **13**, 989.
28 D. Wang, X. Mao, Y. Liang, Y. Cai, T. Tu, S. Zhang, T. Li, L. Fang, Y. Zhou, Z. Wang, Y. Jiang, X. Ye and B. Liang, *Biosensors*, 2023, **13**, 272.
29 U. Saeed, B. Fatima, D. Hussain, R. Ashiq, M. Naeem Ashiq and M. Najam-ul-Haq, *J. Electroanal. Chem.*, 2022, **906**, 115999.
30 T. Chakraborty, M. Das, C. Y. Lin and C. H. Kao, *Mater. Today Chem.*, 2023, **27**, 101273.
31 Z. Saddique, T. Siddique, A. Shehzadi, Q. Ul-Ain, A. Ali, N. Iqbal, A. Mujahid and A. Afzal, *Compos. Commun.*, 2023, **42**, 101673.
32 N. I. Wardani, P. Kanatharana, P. Thavarungkul and W. Limbut, *Talanta*, 2023, **265**, 124769.
33 M. Saeed, Z. Saddique, A. Mujahid and A. Afzal, *Biosens. Bioelectron.*, 2024, **247**, 115899.
34 Y. Li, L. Luo, Y. Kong, S. George, Y. Li, X. Guo, X. Li, E. Yeatman, A. Davenport, Y. Li and B. Li, *Adv. Funct. Mater.*, 2024, **2024**, 2316865.
35 M. A. A. Khushaini, N. H. Azeman, A. G. Ismail, C. H. Teh, M. M. Salleh, A. A. A. Bakar, T. Aziz and A. R. M. Zain, *Sci. Rep.*, 2021, **11**, 23519.
36 B. X. Chen, L. Y. Chen, H. W. Zan, H. F. Meng, C. A. Hsieh, J. B. Yang, M. H. Chen and Y. H. Cheng, *Sens. Actuators, B*, 2022, **361**, 131723.
37 I. Banga, A. Paul, S. Muthukumar and S. Prasad, *ACS Appl. Mater. Interfaces*, 2021, **13**, 16155–16165.
38 I. Banga, A. Paul, V. N. Dhamu, A. H. Ramasubramanya, S. Muthukumar and S. Prasad, *Int. J. Biol. Macromol.*, 2023, **253**, 126894.
39 M. R. O. Vega, Y. Luo, M. Werheid, I. Weidinger, I. Senkovska, J. Grothe and S. Kaskel, *Electrochim. Acta*, 2024, **477**, 143748.
40 N. Promphet, W. Phamonpon, W. Karintrithip, P. Rattanawaleedirojn, K. Saengkiettiyut, Y. Boonyongmaneerat and N. Rodthongkum, *Int. J. Biol. Macromol.*, 2023, **242**, 124757.
41 Y. Liu, Y. Dong, M. Hui, L. Xu, L. Ye, J. Lv, L. Yang and Y. Cui, *Biosens. Bioelectron.*, 2023, **241**, 115699.
42 D. Lee and B. Chua, *Chem. Eng. J.*, 2023, **477**, 146949.
43 D. Lee and B. Chua, *ACS Appl. Mater. Interfaces*, 2021, **13**, 43984–43992.
44 Z. Chen, Z. Xu, T. Qin, D. Wang, S. Zhang, T. Lv, L. Wang, X. Chen, B. Liu and X. Peng, *Sens. Actuators, B*, 2024, **398**, 134687.
45 Y. Liu, G. Yang, T. Li, Y. Deng, Z. Chen and N. He, *Chin. Chem. Lett.*, 2021, **32**, 1957–1962.
46 H. Wang, J. Wang, G. Ma, J. Zhou, L. Du, H. Wu, X. Zhang, Y. He and J. Zhou, *Chem. Eng. J.*, 2023, **464**, 142551.
47 S. Guan, Q. Fu, D. Wang, Y. Han, N. Cao, M. Zhang, H. Shen, R. Yang, B. He, M. Tao, F. Hu, X. Jiang, L. Zheng and B. Situ, *ACS Sens.*, 2022, **7**, 3481–3490.
48 V. Pinrod, W. Chawjiraphan, K. Segkhoonthod, K. Hanchaisri, P. Tantiwathanapong, P. Pinpradup, T. Putnin, D. Pimalai, K. Treerattrakoon, U. Cha'on, S. Anutrakulchai and D. Japrung, *Biosensors*, 2023, **13**, 876.
49 P. Bhatt, D. Kukkar, A. K. Yadav and K. H. Kim, *Spectrochim. Acta, Part A*, 2024, **307**, 123666.
50 P. Bhatt, D. Kukkar and K. H. Kim, *TrAC, Trends Anal. Chem.*, 2024, **173**, 117572.
51 L. A. Pérez-Márquez, M. D. Perretti, R. G. Rodriguez, F. Lahoz and R. Carrillo, *Angew. Chem., Int. Ed.*, 2022, **61**, e202205403.
52 S. Thammajinno, C. Buranachai, P. Kanatharana, P. Thavarungkul and C. Thammakhet-Buranachai, *Spectrochim. Acta, Part A*, 2022, **270**, 120816.
53 G. Song, D. Jiang, J. Wu, X. Sun, M. Deng, L. Wang, C. Hao, J. Shi, H. Liu, Y. Tian and M. Chen, *Chem. Eng. J.*, 2022, **440**, 135979.
54 C. F. Lin, C. H. Chang, L. Noël, B. R. Li, H. F. Meng, O. Soppera and H. W. Zan, *Adv. Mater. Technol.*, 2022, **8**, 2201026.
55 Y. Liu, T. Li, G. Yang, Y. Deng, X. Mou and N. He, *Chin. Chem. Lett.*, 2022, **33**, 1913–1916.
56 S. D. A. Qahtani, H. K. Alzahrani, O. A. Azher, Z. O. Owidah, M. Abualnaja, T. M. Habeebullah and N. M. E. Metwaly, *J. Environ. Chem. Eng.*, 2021, **9**, 105493.
57 N. Passornraprasit, T. Siripongpreda, S. Ninlapruk, N. Rodthongkum and P. Potiyaraj, *Int. J. Biol. Macromol.*, 2022, **213**, 1037–1046.
58 Y. J. Chi, B. Ryu, S. Ahn and W. G. Koh, *Sens. Actuators, B*, 2023, **396**, 134601.
59 U. Nishan, A. Ahmed, N. Muhammad, M. Shah, M. Asad, N. Khan, F. Ullah, R. Ullah, E. A. Ali, H. Nawaz and A. Badshah, *RSC Adv.*, 2024, **14**, 7022–7030.
60 J. Guan, Y. Xiong, M. Wang, Q. Liu and X. Chen, *Sens. Actuators, B*, 2024, **399**, 134842.
61 L. Zheng, D. Zhu, Y. Xiao, X. Zheng and P. Chen, *Biosens. Bioelectron.*, 2023, **237**, 115506.
62 Z. Hu and B. Yan, *ACS Sens.*, 2023, **8**, 4344–4352.
63 S. Chotithammakul, M. B. Cortie and D. Pissuwan, *Biosensors*, 2021, **11**, 209.
64 S. Natarajan, M. C. DeRosa, M. I. Shah and J. Jayaraj, *Sensors*, 2021, **21**, 3178.
65 J. Cheng, Y. Fu, J. Guo and J. Guo, *Sens. Actuators, B*, 2023, **387**, 133795.
66 C. C. Tseng, S. J. Chen, S. Y. Lu, C. H. Ko, J. M. Wang, L. M. Fu and Y. H. Liu, *Chem. Eng. J.*, 2021, **419**, 129592.
67 S. J. Chen, C. C. Tseng, K. H. Huang, Y. C. Chang and L. M. Fu, *Biosensors*, 2022, **12**, 496.
68 C. C. Tseng, S. Y. Lu, S. J. Chen, J. M. Wang, L. M. Fu and Y. H. Wu, *Anal. Chim. Acta*, 2022, **1203**, 339722.
69 F. T. S. M. Ferreira, R. B. R. Mesquita and A. O. S. S. Rangel, *Microchem. J.*, 2023, **193**, 109102.
70 M. M. Bordbar, H. Samadinia, A. Sheini, J. Aboonajmi, M. Javid, H. Sharghi, M. Ghanei and H. Bagheri, *Microchim. Acta*, 2022, **189**, 316.
71 Y. Li, Y. Kong, Y. Hu, Y. Li, R. Asrosa, W. Zhang, B. D. Boruah, A. K. Yetisen, A. Davenport, T. C. Lee and B. Li, *Lab Chip*, 2024, **24**, 2454–2467.
72 X. Chen, Y. Liang, N. Tang, C. Li, Y. Zhang, F. Xu, G. Shi and M. Zhang, *Biosens. Bioelectron.*, 2024, **249**, 1160106.
73 J. F. Diforti, T. Cunningham, E. Piccinini, W. A. Marmisolle, J. M. Piccinini and O. Azzaroni, *Anal. Chem.*, 2024, **96**, 5832–5842.

© 2024 The Author(s). Published by the Royal Society of Chemistry